

Formation of fine near-field scanning optical microscopy tips. Part I. By static and dynamic chemical etching

Alexander Lazarev, Nicholas Fang, Qi Luo, and Xiang Zhang^{a)}

Department of Mechanical and Aerospace Engineering, University of California at Los Angeles, 420 Westwood Plaza, Los Angeles, California 90095

(Received 7 November 2002; accepted 12 May 2003)

The probe tip is the key component in scanning probe microscopes and their applications in the nanoscale imaging and nanofabrication. In this work, we have investigated the formation of near-field scanning optical microscopy probe tips from optical fiber by chemical etching. Static and dynamic etchings and their combinations are studied. The etching process is optimized, and tips with short tapers, small apertures (about 50 nm) and large aperture cone angles (40°) are successfully obtained. Multiple-tapered tips are also fabricated by using different dynamic regimes. It is found that the taper profiles are determined by the nonlinear dynamic evolution of the meniscus of the etchant near the fiber. © 2003 American Institute of Physics. [DOI: 10.1063/1.1589583]

I. INTRODUCTION

Recently, near-field scanning optical microscopy and its variations, which combine the scanning probe technology with optical microscopy, have been intensively applied in the study of material science,¹ biology,² nano-optics,³ and nanofabrications.^{4,5} These techniques utilize a sharp tip to scan across the sample surface to deliver or collect light from the sample. The configuration of the tip in these applications is of utmost importance to the performance of the systems. The tip, which is normally coated with a metal, works as the probe as well as light waveguide. It has a complex loss mechanism. While approaching the apex, the diameter of the tip becomes smaller. The cutoff diameter, at which the lowest guided mode exists, is a very important feature of the metallic waveguide. Below the cutoff diameter, the intensity of the light exponentially decreases. With respect to the transmission efficiency the distance between the cutoff diameter and the apex—the cone angle, is the most crucial parameter of the tip.

The cone angle of the sharpened tip greatly affects the performance of the tip in terms of its light transmission.⁶ Large transmission is achievable with large cone angle. For example, transmission of 10^{-3} has been obtained through tips with cone angle of 40°. ⁷ In addition to cone angle, the tapered profile of the tip is also important. Saiki fabricated tips with double tapered apex,⁸ and Tatsui developed a process to make triple-tapered tips that improves the light transmission.⁹ Sqalli attached a gold particle to the probe apex and studied the surface plasmon resonance between the gold particle and the sample surface, which has been shown to improve the resolution for the near-field microscopy.¹⁰

Great effort has been devoted to tip probe fabrication. The fabrication process typically includes two steps: formation of a transparent tapered probe with a sharp apex, and metal coating of the probe to form a transmissive aperture at

the apex. The methods to fabricate the tip can be categorized into three groups: chemical etching,^{11–13} laser heating and pulling,¹⁴ others methods include crystal growth¹⁵ and carbon nano tube.¹⁶ Among them, chemical etching is most intensively studied. Various etching based methods to produce different configurations of fine optical fiber tips have been proposed in the literature. The most successful one is HF static etching.^{11–13} While a bared fiber is dipped into a two phase fluid, HF solution, which serves as etchant, and an organic protecting solvent, a meniscus of the HF solution is formed due to the surface tension difference between the HF solution and the solvent [Fig. 1(A)]. The evolution of the meniscus leads to the tip formation. As the fiber is gradually etched away, the products of the chemical reaction flow down since the products are heavier than the acid. The flow affects the etching rates at different depths. Now the newly etched volume is a part of the meniscus system; it is filled with acid and the products of the chemical reaction. This leads to an increasing weight of the liquid of the meniscus [Fig. 1(B)]. At some point the weight of the liquid raised by the meniscus reaches a threshold value which exceeds the amount of the surface tension force, the meniscus then drops down to the next stable point where the amount of the surface tension force, at the new contacting angle, can balance out the weight of the liquid of the new meniscus [Fig. 1(C)].

The etched out fiber surface which was in contact with the HF solution is now in contact with the solvent. The solvent protects it from further attacking by the HF acid. This process continues until the taper is completely formed and the meniscus disappears. We refer this process as static etching, since the fiber is stationary during the process.

For a given fiber, using different protective solvents, which alter the surface tension of the acid/solvent interface and the contacting angle of that interface to the fiber, could change the final tip shape. As reported in Ref. 13, etching system with Isooctane protective layer produces cone angles of 40°, while that with Toluene results in 29°. However, a clear trend has not yet been identified since solvents with

^{a)}Author to whom correspondence should be addressed; electronic mail: xiang@seas.ucla.edu

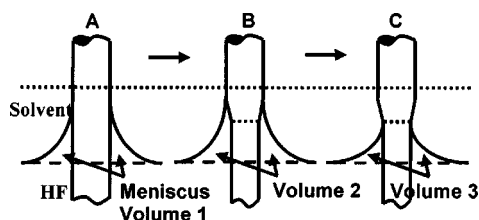


FIG. 1. Taper formation due to meniscus based etching process. The force balance is broken in step B due to etching of the fiber tip, which leads to recession of the meniscus to the new position in step C.

similar parameters, such as 1-Octanethiol and Toluene (density=0.843 and 0.867 g/cm³, respectively, and surface tension=28.02 and 28.4 dyn/cm, respectively) may result in very different cone angles: 41° and 29°, respectively.

There are some other etching methods that can be categorized into static etching. One utilizes different etching rates of different layers in the fiber.¹⁷ Another utilizes a multi-step etching procedure including coating of the tip with a polymer to partially protect it from the acid at an intermediate step.¹⁸ There is also the so-called “tube” etching method, wherein the fiber is dipped into HF acid without stripping the polymer coating.^{19,20}

In contrast to the static etching, wherein the fiber does not move vertically during the etching procedure, a dynamic etching method is also introduced.⁷ It is still a meniscus based technique, yet introduces a new feature: moving the fiber vertically while immersed in the etchant. The idea here is to alter the recession speed of the meniscus (as it happens in the static etching process) by moving the fiber either up or down at certain speed, constant or not, hence the name dynamic. The speed determines the amount of time that the cross section of the fiber at each height is exposed to the acid, and therefore how far the fiber will be etched laterally at that height.

This work presents a detailed investigation on formation of sensing tips based on the static and dynamic etching methods.

II. EXPERIMENT

In our experimental setup, fibers were held in the fiber rack, which was mounted on the translational *z* stage. A set of up to nine fibers can be etched at the same time. Cuvettes with acid and solvent inside were placed in the stationary cuvette holder. Each fiber was etched in an individual cuvette. By moving the *z* stage vertically, the fibers were dipped into or withdrawn from the cuvettes according to the desired dynamic regime. After the etching was completed, fibers were pulled out and dipped into the de-ionized water baths for rinsing. This ensures that the tips are not altered by residual etchant. After rinsing, fibers were pulled out of the fiber rack and individually cleaned by dipping them into methanol bath.

Three types of fibers have been used: single-mode fiber QSMF-320-2/125-0.25-L, multimode fiber FVP1001110125 (both from Polymicro Technologies), and multimode fiber GIF 50 ultraviolet (UV) from Thorlabs. They are all UV fibers since we are targeting applications at UV range. Be-

fore etching, the protective coating layers of the fibers were stripped off by either mechanical stripping or hot (100 °C) sulfuric acid etching depending on the type of the polymer coatings. We used HF acid as etchant. High concentration HF acid is favorable, since it reduces the total etching time, as well as reducing the adverse effect of HF diffusing into the solvent layer and thus attacking the fiber above the HF/solvent interface. Concentration of HF in the herein experiments was 48%. We used silicon oil as the immiscible protective solvent that stays above the HF acid.

Charge coupled device cameras and high magnification optics were utilized to *in situ* observe and record the etching process. For this purpose, HF acid and silicon oil were placed in a transparent polystyrene cuvette, which is resistant to HF acid and silicon oil. The observation helped to understand the dynamics of the acid meniscus evolution during the etching process, and the main phenomena at work.

Most of the experiments were performed with the multimode UV-grade fiber FVP1001110125 from Polymicro Technologies. These fibers feature 100 μm core diameter and about 10 μm cladding thickness. This favors a uniform etching rate, since most of the time is spent on etching the uniform core material. Multimode fibers have two unique properties compared to single mode fibers. The first one is the high damage threshold while delivering high intensity UV light. The typical threshold of UV single mode fiber is kW, while UV multimode fibers can survive in MW; although there is more attenuation to the total input energy while using multimode fiber, higher output energy can be obtained by using much more input power without damage. The second one is the high light collecting efficiency. The light collecting efficiency using multimode fiber tips can be much higher than that using single mode fiber tips.²¹

III. RESULTS AND DISCUSSION

Before we investigated the dynamic etching regimes, we first studied the static etching of each fiber type. The experiments show that the Multimode fiber FVP1001110125 is the most suitable fiber for further etching experiments. The tips made from single mode fiber QSMF-320-2/125-0.25-L and multimode GIF 50UV yielded some unexpected negative features, and were not used in further experiments. The typical tips made from the above mentioned three types of fibers by static etching are shown in Fig. 2. GIF 50UV featured uneven surface quality [Fig. 2(a)] and poor reproducibility. QSMF-320-2/125-0.25-L yielded blunt tips [Fig. 2(b)]. Its core was 2 μm in diameter, and was not tapered as well as those of the other fibers. On the other hand FVP1001110125 performed very well [Fig. 2(c)]. The experimental conditions and results are listed as follows. Static etching times for GIF 50UV and QSMF-320-2/125-0.25-L were about 35–40 min and 1 h, respectively, resulting in tapers of 32°/180 μm and 37°/170 μm, respectively. The etching time for FVP1001110125 was about 30 min, resulting in taper of 28°/250 μm, and an apex diameter of less than 100 nm.

We chose FVP1001110125 for further investigation on dynamic etching. In order to investigate the process of dynamic etching, a series of experiments have been carried out.

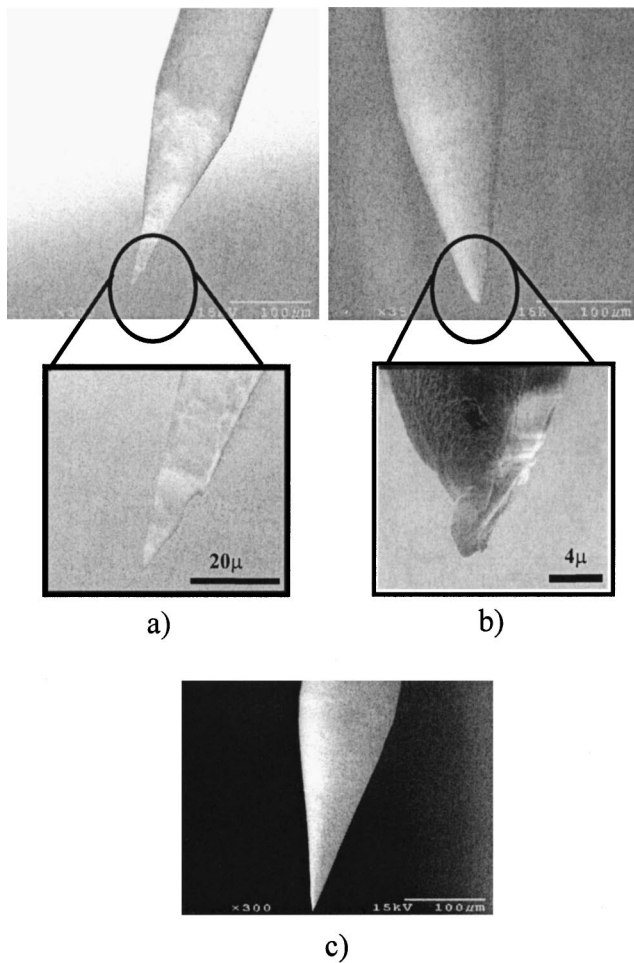


FIG. 2. SEM images of the tips made by static etching: (a) tips made from multimode fiber GIF 50UV, (b) single mode fiber QSMF-320-2/125-0.25-L, and (c) multimode fiber FVP1001110125.

We first performed the experiments combining the dynamic and static etching, wherein the fiber was first etched for varying time intervals while moving at a chosen speed; then etched statically for the remaining time until the etching is finished. The meniscus-based static etching is a self-terminating process, while the dynamic etching with fiber moving downward needs to be terminated by hand after the tip aperture is formed. Varying the dynamic etching time length allows one to experimentally determine the exact time needed to complete the etching process in dynamic mode, and to examine the progression of the dynamic etching, as

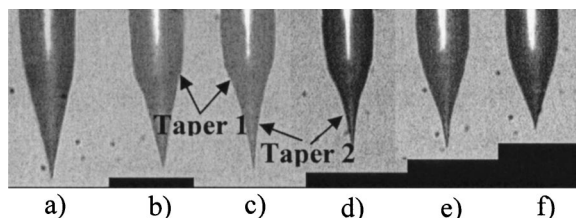


FIG. 3. SEM images of the tips etched with different dynamic regimes. The dynamic etching time was varied (all): (a) 0 min (all static), (b) 7 min, (c) 9 min, (d) 12 min, (e) 18 min, and (f) 20 min. Fibers were moved at 6.67 $\mu\text{m}/\text{min}$ at dynamic etching regimes.

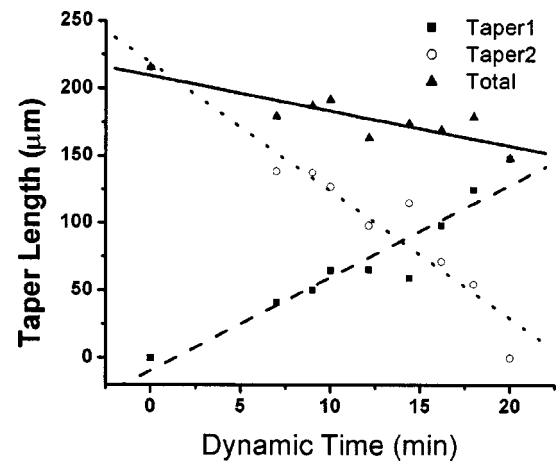


FIG. 4. Taper lengths of different portions in tips made by mixed etching method: (taper 1) corresponding to the dynamic regime and (taper 2) corresponding to the static regime. Fiber speed was 6.67 $\mu\text{m}/\text{min}$ in the dynamic regime.

well as to distinguish the taper differences between dynamic and static regimes.

Figure 3 shows the tips following this procedure at various dynamic etching times from 0 [Fig. 3(a), all static etching] to 20 min [Fig. 3(f), all dynamic etching] with fiber downward moving speed of 6.67 $\mu\text{m}/\text{min}$ in the dynamic regimes. It can be seen that the tips form two tapered regions, corresponding to dynamic and static etching regimes. As expected, while increasing the dynamic etching time, the taper length corresponding to the dynamic regime increases; that corresponding to the static regime decreases, and the total decreases. The results are shown in Fig. 4.

It can also be seen from Fig. 3 that the cone angle of the tip obtained in this particular acid-solvent-fiber system varies in different etching regions. The taper cone angle of the dynamic region is larger than that of the static region, which is the residue cone angle of the tip aperture; and that of the static region decreases slightly with the increase of the dynamic etching time. For further visualization, the contours of the fibers have been digitized, and the corresponding residual cone angles are calculated and plotted in Fig. 5. We see a slight decrease of the residue cone angle with the increase of dynamic etching time. Here the cone angle of the tip in the

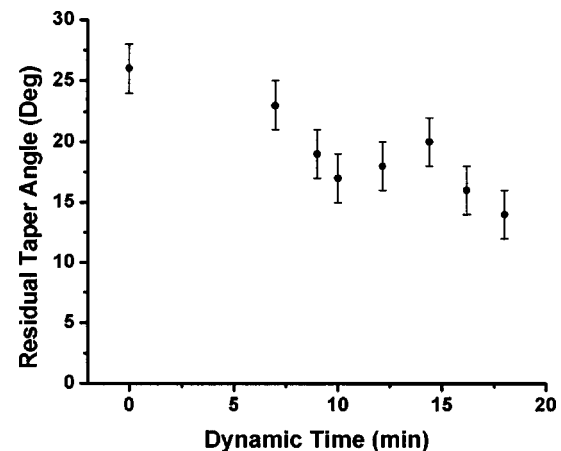


FIG. 5. Residual taper cone angles vs dynamic etching times.

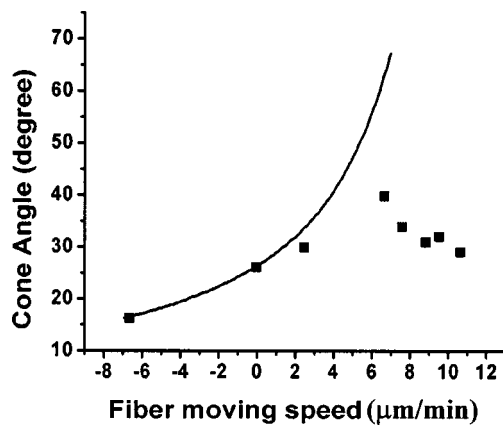


FIG. 6. Taper angles vs the fiber moving speed: (■) experimental results; (solid curve) modeling result from Ref. 21. Fiber FVP1001110125 is used. Positive fiber speed corresponds to downward moving, yet the negative speed the upward moving.

all-dynamic etching [Fig. 3(f)] is not included, which is 40° , the largest cone angle we have obtained in this etching system.

The above experiments show that dynamic etching with fiber moving down can provide larger cone angles. Based on this, we carried out etching experiments with fiber moving down at different speeds. The results are shown in Fig. 6. For comparison, we have also performed experiments with fiber moving up at different speeds. The results show large deviations from the model proposed by Mononobe²² in the case of downward motion of the fiber; while in the upward motion case (negative speed) the experimental results followed the simple model rather well.

It is shown that in downward moving case, the cone angle increases with the fiber moving speed until it reaches $6.67 \mu\text{m}/\text{min}$, when the largest cone angles of 40° are achieved. Subsequently the cone angle decreases slightly. Moreover, our experiments show that at very large dipping speeds, the fibers are slightly etched above the top of the taper. Examples of such tips are shown in Figs. 7(d) and 7(e). Because the dipping speed is so large, the contacting line of the meniscus to the fiber creeps up at the beginning of the etching. This will be discussed at the end of this section. For reference, other tips with different fiber dipping speeds are also shown here [Figs. 7(a)–7(c)].

We fabricated several tips with large cone angles and small apertures. Figure 8 shows two scanning electron microscope (SEM) images of such tips obtained at fiber speeds

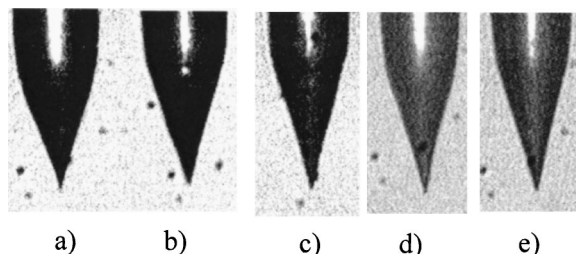


FIG. 7. Tips obtained with fiber moving speeds above $6.67 \mu\text{m}/\text{min}$: (a) $6.67 \mu\text{m}/\text{min}$, (b) $7.62 \mu\text{m}/\text{min}$, (c) $8.89 \mu\text{m}/\text{min}$, (d) $9.52 \mu\text{m}/\text{min}$, and (e) $10.7 \mu\text{m}/\text{min}$.

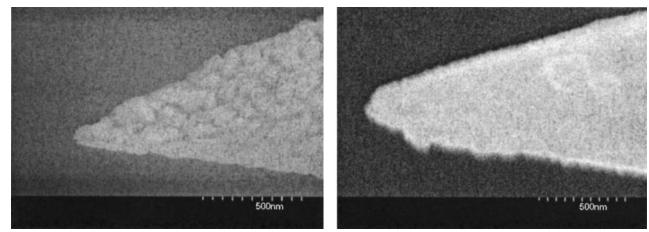


FIG. 8. SEM images of etched tips. Fiber moving speed is $6.67 \mu\text{m}/\text{min}$.

of $6.67 \mu\text{m}/\text{min}$. Apertures of these two tips have been closed by the silver coating. However, taking into account the thickness of the silver coating, the apertures of the tip in the left image should be around 50 nm.

Experiments with variable fiber speeds during the process were also carried out to obtain multiple-tapered tips. Figure 9 illustrates an example of a tip made by such a process. The tip was first etched 5 min with fiber moving up at a speed of $6.67 \mu\text{m}/\text{min}$, followed with static etching of 10 min, and then finished by dynamic etching of 8.5 min with fiber moving down at a speed of $7.62 \mu\text{m}/\text{min}$. The taper shows three discrete sections corresponding to the above three etching steps with different fiber moving speeds. The residual cone angle of the apex is about 40° .

Further investigation of this process in conjunction with *in situ* observation has revealed the dynamics of this system. It was found that the meniscus does not slide down the fiber gradually; instead it jumps down in step of about $5 \mu\text{m}$ at a time. This could be explained by the presence of some “stiction” factor of the surface tension force, which allows the meniscus to stay attached to one contact line until the force imbalance is great enough to overcome this stiction force.

Our experiments also show that in all-static or all-dynamic etching, the taper profile is not linear. This can be seen from the tips in Figs. 2(c), 3(a), and 7(a). In each tip, the local taper angle gradually decreases while approaching the tip apex. This indicates that the meniscus decreases at an irregular speed during the etching process: slow at the beginning (V_1) and faster toward the end (V_2). So, if in dynamic etching mode, the fiber is moving downward at some speed V between V_1 and V_2 ($V_1 < V < V_2$), then relative to the fiber surface, the meniscus may move upward first, then down-

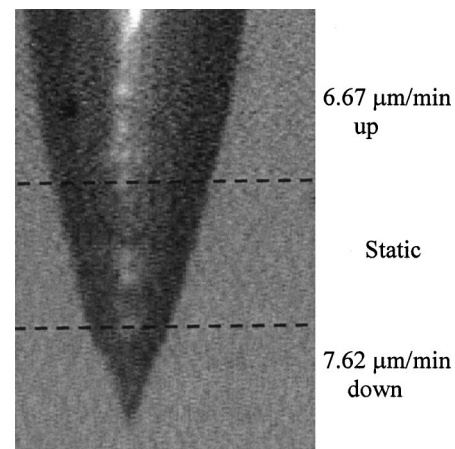


FIG. 9. Tip made with varying fiber moving speed.

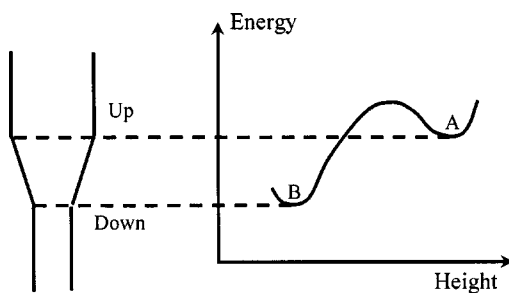


FIG. 10. Qualitative representation of meniscus energy states. Meniscus tends to stay either in the upper or lower position and is unstable in between.

ward due to further recession. This can explain why in Figs. 7(d) and 7(e) the areas above the tapers are also slightly etched.

Meniscus behavior could be qualitatively described as illustrated in Fig 10, where there are two stable positions: up position, in contact with the joint line of the taper and the original diameter of the fiber (or an intermediate position in the middle of the process), corresponding to low energy point (A); and down position, transitioning from the tapered region to the remaining cylindrical region, corresponding to another low energy point (B). The meniscus tends to stay at these two positions rather than at a place between them. This explains why the meniscus jumps rather than transitioning smoothly. To explain the nonlinearity of the meniscus evolution, hence the nonlinearity of the taper profile, an effective dynamic model is needed.

ACKNOWLEDGMENTS

This research was supported by National Science Foundation (NSF) (Grant No. DMI-0218273), Office of Naval Research (ONR), Young Investigator award (Grant No. N00014-02-1-0224), and National Science Foundation (NSF) CAREER Award (No. DMI 9703426).

- ¹H. F. Hess, E. Betzig, T. D. Harris, L. N. Pfeiffer, and K. W. West, *Science* **264**, 1740 (1994).
- ²R. C. Dunn, G. R. Holtom, L. Mets, and X. S. Xie, *J. Phys. Chem.* **98**, 3094 (1994).
- ³For a review, see J. E. Sipe and R. W. Boyd, *Top. Appl. Phys.* **82**, 1 (2002).
- ⁴I. Smolyaninov, D. Mazzoni, and C. Davis, *Appl. Phys. Lett.* **67**, 3859 (1995).
- ⁵L. Ghislain, V. Elings, K. Crozier, S. Manalis, S. Minne, K. Wilder, G. Kino, and C. Quate, *Appl. Phys. Lett.* **74**, 501 (1999).
- ⁶B. Hechet, B. Sick, U. P. Wild, V. Deckert, R. Zenobi, O. J. F. Martin, and D. W. Pohl, *J. Chem. Phys.* **112**, 7761 (2000).
- ⁷H. Muramatsu, K. Homma, N. Chiba, N. Yamamoto, and A. Egawa, *J. Microsc.* **194**, 383 (1999).
- ⁸T. Saiki, S. Mononobe, and M. Ohtsu, *Appl. Phys. Lett.* **68**, 2612 (1996).
- ⁹T. Yatsui, M. Kouroggi, and M. Ohtsu, *Appl. Phys. Lett.* **73**, 2090 (1998).
- ¹⁰O. Sqalli, I. Utke, P. Hoffmann, and F. Marquis-Weible, *J. Appl. Phys.* **92**, 1078 (2002).
- ¹¹B. A. Puygranier and P. Dawson, *Ultramicroscopy* **85**, 235 (2000).
- ¹²A. Sarah, C. Philipona, P. Labelet, M. Pfeffer, and F. Marquis-Weible, *Ultramicroscopy* **71**, 59 (1998).
- ¹³P. Hoffmann, B. Dutoit, and R.-P. Salathe, *Ultramicroscopy* **61**, 165 (1995).
- ¹⁴N. Essaidi, Y. Chen, V. Kottler, E. Cambriel, C. Mayeux, N. Ronarch, and C. Vieu, *Appl. Opt.* **37**, 609 (1998).
- ¹⁵E. Oesterschulze, W. Scholz, Ch. Mihalcea, D. Albert, B. Sobisch, and W. Kulisch, *Appl. Phys. Lett.* **70**, 435 (1997).
- ¹⁶C. Cheung, J. Hafner, T. Odom, K. Kim, and C. Lieber, *Appl. Phys. Lett.* **76**, 3136 (2000).
- ¹⁷S. Mononobe, T. Saiki, T. Suzuki, S. Koshihara, and M. Otsu, *Opt. Commun.* **146**, 45 (1998).
- ¹⁸S. Mononobe, M. Naya, T. Saiki, and M. Otsu, *Appl. Phys.* **36**, 1496 (1997).
- ¹⁹R. Stockle, C. Fokas, V. Deckert, R. Zenobi, B. Sick, B. Hecht, and U. Wild, *Appl. Phys. Lett.* **75**, 160 (1999).
- ²⁰P. Labelet, A. Sayah, M. Pfeffer, C. Philipona, and F. Marquis-Weible, *Appl. Opt.* **37**, 31 (1998).
- ²¹F. de Fornel, *Evanescent Waves from Newtonian Optics to Atomic Optics*, 1st ed. (Springer, Berlin, 2001), p. 200.
- ²²S. Mononobe and M. Ohtsu, *J. Lightwave Technol.* **14**, 2231 (1996).